Indian Journal of Geo-Marine Sciences
Vol. 39(4), December 2010, pp. 579-588

Dynamic pressure and run-up on curved seawalls compared with vertical wall under cnoidal waves

V Sundar & K V Anand

Department of Ocean Engineering, Indian Institute of Technology Madras, Chennai, India.

[E-mail: vsundar@iitm.ac.in]

Received 20 August 2010; revised 21 December 2010

Seawalls are the most widely adopted coastal protection measure. The design of an efficient seawall should be such that overtopping is minimized even during coastal flooding and extreme events by maintaining its crest elevation lower. This may possibly be achieved by reshaping the front shape of the structure in such a way that it offers maximum resistance to the flow or enhances the dissipation of incident wave energy. With this background, an experimental study on the measurement of run-up and dynamic pressures over three different types of curved front face seawall models along with a vertical seawall was carried out. The measured parameters for the three types of curved seawalls are compared with that for a vertical seawall. All the tests were carried out with the models rigidly fixed over a bed slope of 1 in 30 in a wave flume and subjected to the action of Cnoidal waves. The dynamic pressure distributions measured along the surface and the run-up over the models are reported in a dimensionless form as a function of relative water depth and ursell parameter. The details of the test facility, models, experimental program, results and analysis are presented and discussed in this paper.

[Keywords: Curved seawall, Regular waves, Dynamic pressures, Run-up, Relative water depth**]**

Introduction

Apart from the coastal erosion and rise in sea level natural coastal hazards like storm surge and tsunami are affecting particularly, the densely populated areas resulting in loss of life and property. It is evident that a seawall as a coastal protection measure should be effective with an optimum use of the coastal space, with less or no wave overtopping by maintaining a lower crest elevation.

Seawall depending on the shape of its surface facing the ocean waves can further be classified as vertical, sloping, curved or stepped. The dissipation of the incident energy when waves act on a sea wall is mostly due to it run-up and reflection. In the case of vertical walls, the amplitude of the waves near the wall magnifies to a maximum extent of twice the incident wave height that promotes scour near its toe and thereby questioning its stability. In order to dissipate the incident wave energy gradually through shoaling, sloping walls were introduced. Although more stable[1-2], reported that the impact pressures and run-up on sloping walls are greater than those on vertical walls thus requiring higher crest elevation and further it occupies more space compared to that of a vertical seawall. Hence, it is evident that this objective may be achieved by considering a curved front shape of the structure as a compromise, although the pressures exerted on such type walls are slightly higher compared to that on vertical walls. Weber[3] has given a conceptual design of curved seawall with a combination of a parabolic and a circular arc which brings a smooth change in the direction of propagation from horizontal to vertical and vise versa to reduce the wave induced pressures. Murakami *et al*.[4] proposed a new type of circular arc non over topping seawall and measured the pressures and forces due to regular waves. It was concluded that the critical crest elevation was much less compared to that for a vertical seawall. The pressures were reported to be a function of the ratio of water depth, d to wave height, H with its maximum occurring closer to the still water level, SWL. Kamikubo *et al*.[5] investigated the characteristics of the curved seawall and the fluid flow near the seawall was reproduced through numerical simulation using finite volume method. The results obtained were almost similar to that of Murakami[4]. Similar study was reported by Kamikubo[6] and investigated the spray when the waves strike the wall. Murakami[7] reported the efficiency of a curved seawall under increased water level due to global warming. The literature review revealed that a variety of configurations of curved sea

front walls have been attempted, some of which have also found its application in the field. However, most studies are limited to the action of regular or random waves. The post great tsunami has added a new dimension to the problem of the response of such structures exposed to the action of shallow water waves like the solitary and Cnoidal waves as they represent closely the characteristics of a tsunami. This prompted the investigators to undertake the present study.

Materials and Methods

Experimental Investigations

The tests have been carried out in a 72.5 m long and 2 m wide wave flume in Department of Ocean Engineering, IIT Madras, by adopting a model scale of 1:5. The models considered for the study are, vertical wall (model-VW), the seaside front face of curved front seawall (model-GS) was a combination of two radii of curvature as suggested[8] by US Army Corps of Engineers that was adopted at Galveston, Texas, USA, during 1905. The model is a modified version of the model proposed by Kamikubo *et al*.[5] The cross-section of the seawall model proposed by Kamikubo *et al*.[5] was formed with the deepest point from its base and from the vertical joining its toe and the crest of the wall are around 40% and 50% of its height respectively. The pressure experienced by such a wall is reported as some 3 to 4 times more than that on a vertical wall, and hence for the present study a modified section with the deepest point from the vertical joining its toe and the crest of the wall as 40% of its height was considered. The curved front seawall was thus formed by adopting nine varying radii increasing from bottom towards top and referred to as (model-FSS). The other model (model-CPS) considered is a curved front seawall from the concepts of Weber[3], which consists of a parabolic curve at the bottom with a quarter circle at the re-curved portion which was connected smoothly at the intersection. The geometries of all the curved front seawall models considered under the present study are projected in Fig. 1.

Three curved front face seawall models along with a vertical seawall model are made of fiber reinforced polymer were rigidly fixed over a bed slope of 1 in 30. Two different water depths of 0.88 m and 1 m were employed for the tests. The curvatures along with the locations of the pressure ports are presented in Fig. 2. The pressure transducers are mounted on the models along its depth such that the depth of submergence of the pressure port, z/d (z is depth below still water and d is water depth) is the same. The wave gauges are placed at appropriate positions to capture the time history of the composite water surface elevation. Similar to the principle of the wave gauge, the run-up probe was fabricated to measure the run-up on the seawalls. The run-up probe consists of two parallel stainless steel wires of 1 mm diameter spaced 10 mm apart and are fixed along the surface of the seawalls. When immersed in water, the electrodes measure the conductivity of the instantaneous volume of water between them. The conductivity change is linearly proportional to the variation in the water surface elevation for vertical seawall and non-linearly proportional for curved front seawalls, since the length of surface will not be varying linearly with the depth of water. For this a polynomial equation is fitted to the calibration curve of each curved seawall. The models are placed at the farther end of from the wave maker over the rigid sloping bed. Arrangements were made to test two models simultaneously, by placing a partition wall along the length of the flume over the adopted bed slope. The experimental set-up along with the locations of the wave gauges and the model is shown in Fig. 3. The sections were exposed to the action of Cnoidal waves with period ranging between 3 and 12 sec, each of which was associated with a wave height of 0.05 m, 0.1 m and 0.15 m, thus covering a wide range of Ursell's parameter ($U_r = LH^2/d^3$) from 3.6 to 362. Herein, *L, H* and *d* are the wavelength, wave height and water depth respectively.

Results and Discussion

Dynamic pressures

Typical variations of the dimensionless shoreward peak pressures, ($p_{sh}/\gamma H$), (where p_{sh} – shoreward peak pressure, γ - specific weight of water and *H* is the wave height) along the relative depth of the wall, *z/d* (z - point of measurement of pressures along the surface, defined negative below Still Water level, SW) for U_r ranges of 3.6-112.3, 7.3-232.8 and 11-229.1 are projected in Fig. 4(a), 4(b) and 4(c) respectively. The pressure exerted by long waves are greater, is clearly reflected in the results. The results exhibit a pressure decay along the depth closer to the bed for $z/d < -0.25$, is observed to be more for models (GS) and (CPS) than for models (VW) and (FSS). This is due to the nature of the curvature of models (GS) and (CPS), being more flat near the bottom, in which case, the bottom port of the seawall acts nearly

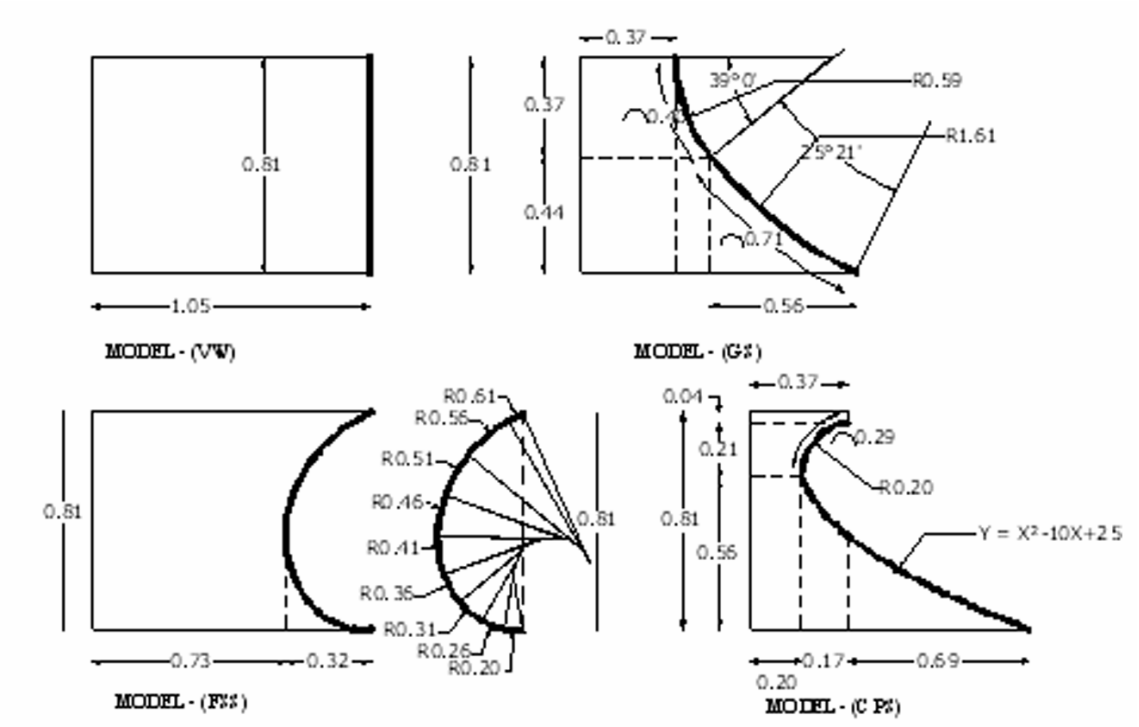

Fig. 1—The geometry of the curved front seawalls.

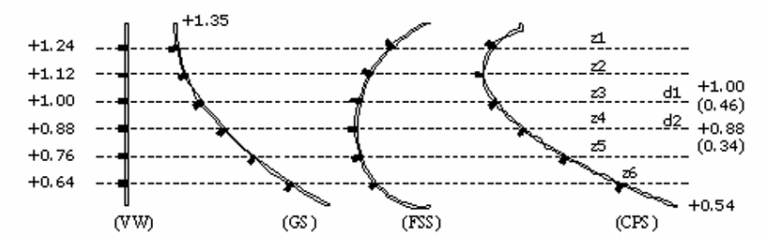

Fig. 2—The models (VW) (GS) (FSS) and (CPS) along with the locations of the pressure ports.

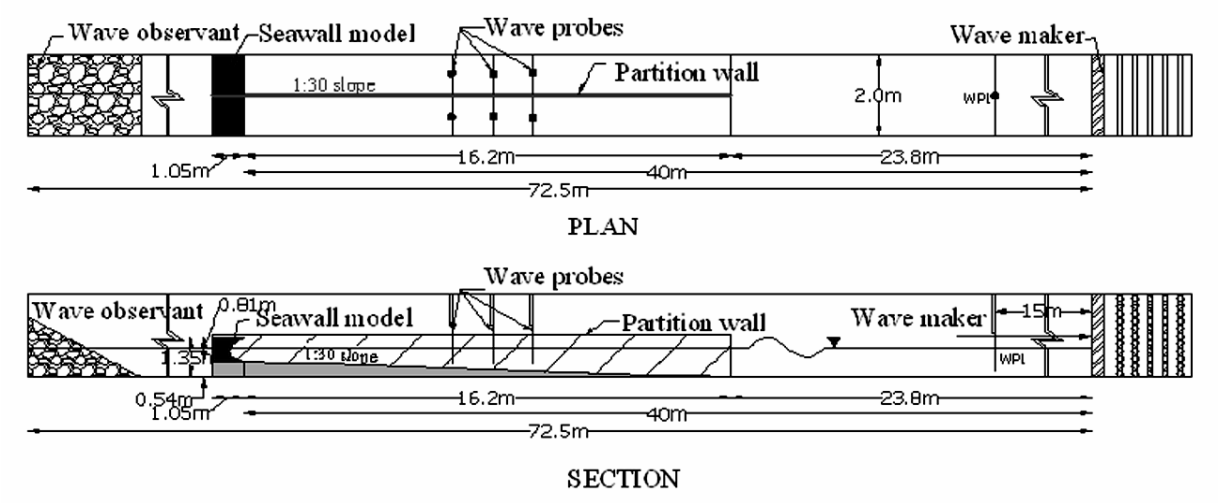

Fig. 3—The plan and sectional view of the models positioned in the wave flume.

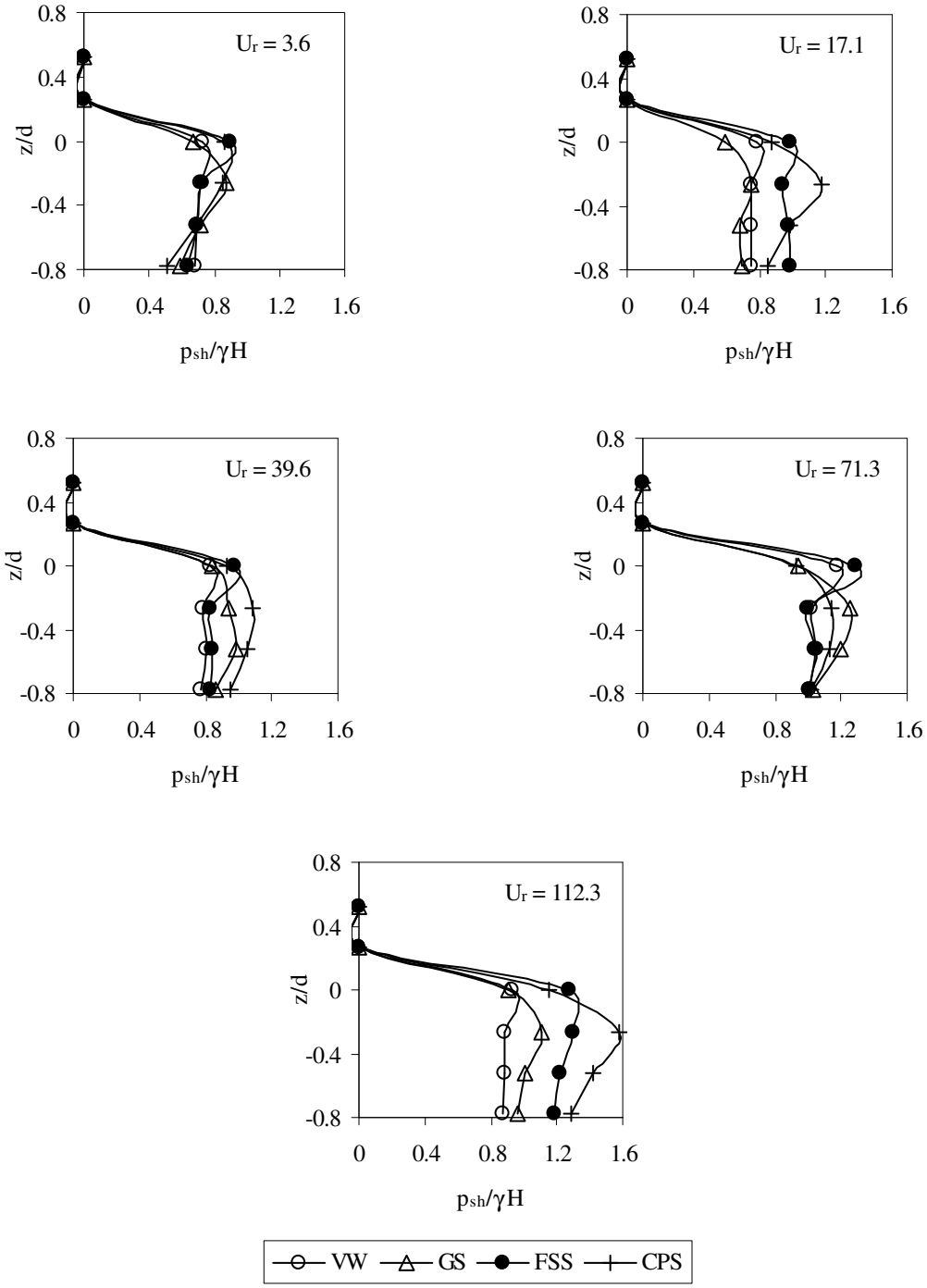

Fig. 4(a)—wave pressure distribution for $H/d = 0.108$ for various U_r

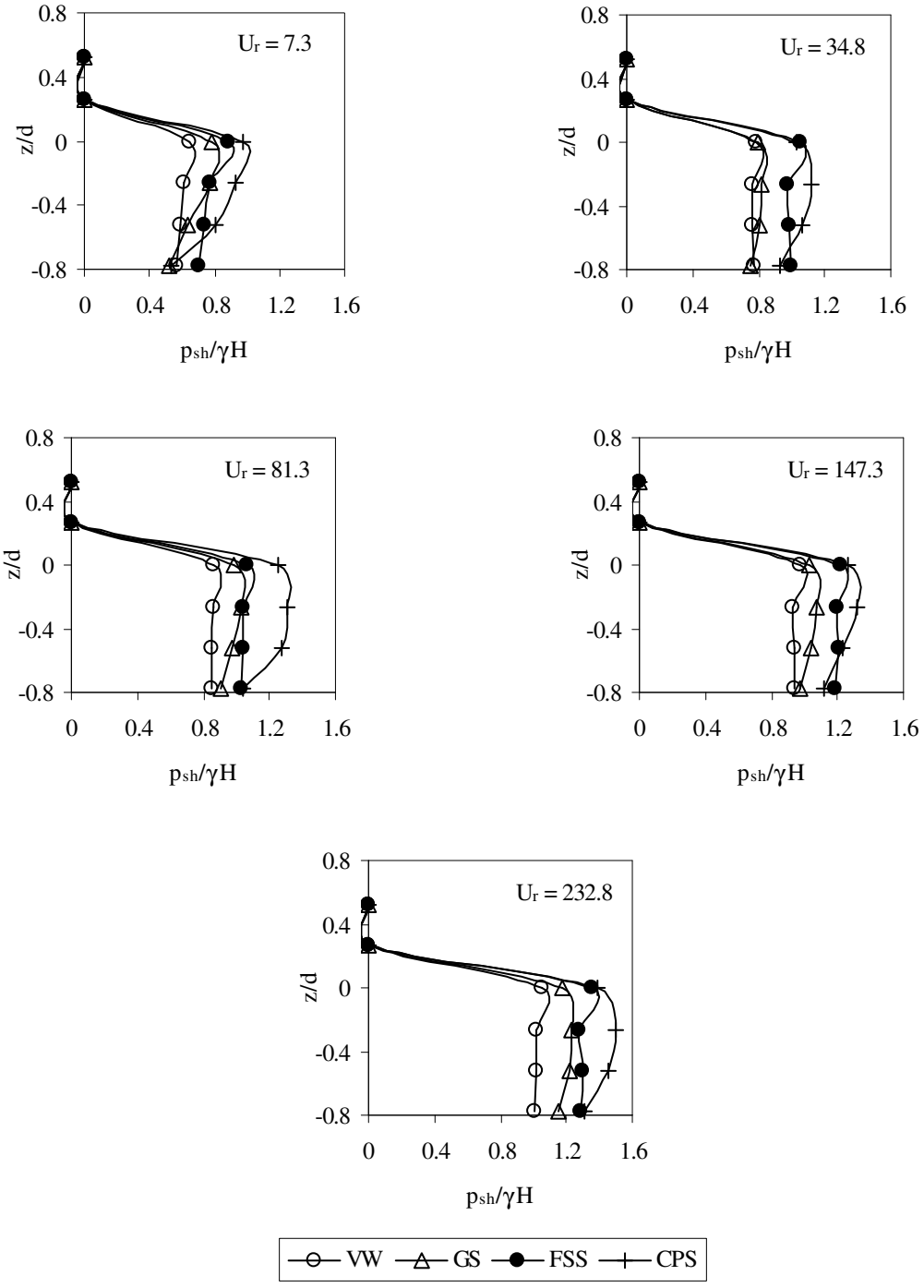

Fig. 4(b)—wave pressure distribution for $H/d = 0.217$ for various U_r

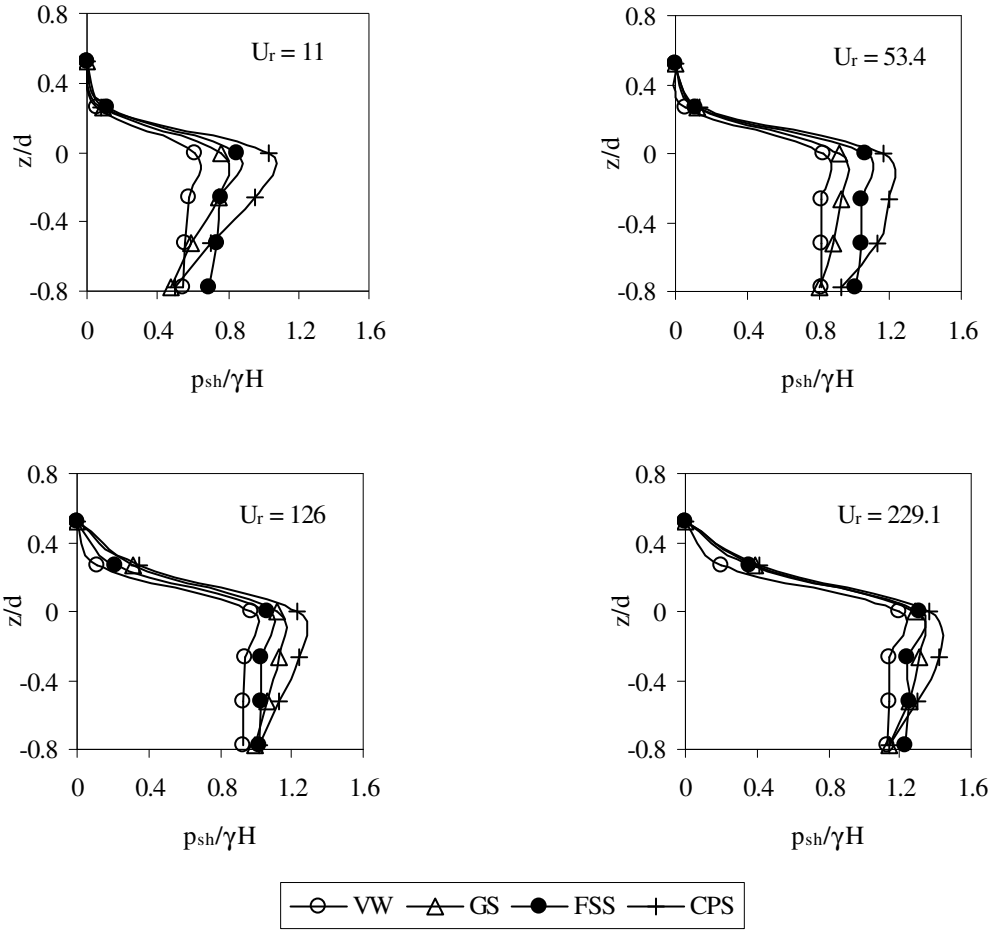

Fig. 4(c)— wave pressure distribution for H/d = 0.326 for various U_r

as a horizontal bottom where the exerted dynamic pressure is less. Hence, it experiences less pressure. Among the models (GS), (FSS) and (CPS), the CPS model is found to experience more pressure than the other models (GS) and (FSS) for most of the U_r ranges considered herein.

The next exercise is to compare the intensity of pressures on the different shaped walls with that exerted on a vertical wall. This is done by obtaining the percentage difference in pressures, with vertical seawall to other three models (GS) (FSS) and (CPS) for a particular z/d, d/L and U_r as:

$$P^* = [\{p_{sh} \text{ on model } (GS \text{ or } FSS \text{ or } CPS) - p_{sh} \text{ on model } (VW)\}/p_{sh} \text{ on model } (VW)] \times 100 \quad \ldots(1)$$

The variation of p^* for model (GS) as a function of d/L for U_r range of 3.6 - 229.1 and z/d = 0.0, –0.26, –0.52 and –0.78 are shown in Fig. 5. The pressure on the model (GS) is found to be higher than that on model (VW) near the free surface. For locations closer to the bed z/d < –0.5 a reverse trend is seen, that is the pressure on model (VW) is higher than on model (GS). This is due to the nature of the curvature of model (GS), being more flat at the said locations. At z/d = –0.26, the maximum percentage increase in the pressures on models (GS) compared to for model (VW) occurs at lower d/L for all the H/d ratios, to a maximum extent of about 28%.

The variation of p* for model (FSS) as a function of d/L for U_r range of 3.6 - 229.1 and z/d = 0.0, –0.26, –0.52 and –0.78 are shown in Fig. 6. The pressure on the model (FSS) is found to be higher than on model (VW) for all the relative pressure port locations, z/d considered. At z/d = –0.26, the maximum increase in p* for model (FSS), compared to model (VW) at lower d/L of 0.014 for U_r range of 3.6 - 112.3 is observed to be about 47 %. As also stated by

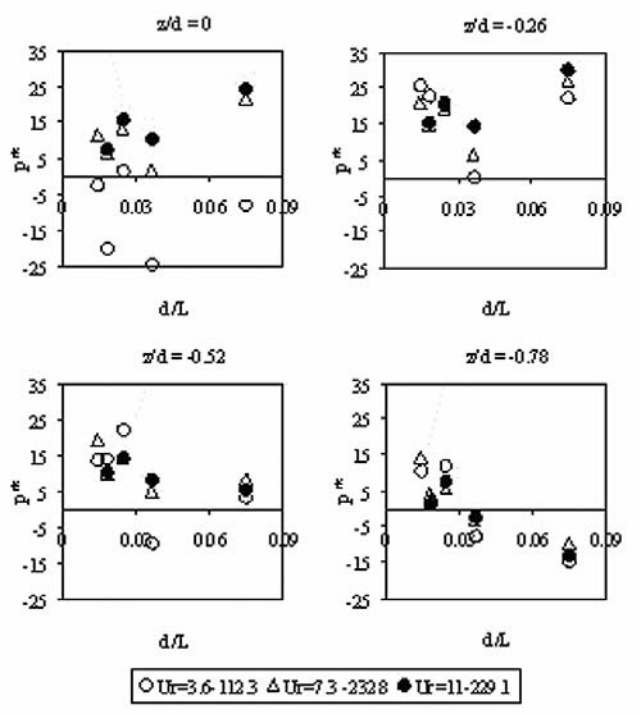

Fig. 5—p* distribution of model (GS) for various *d/L* and U_r.

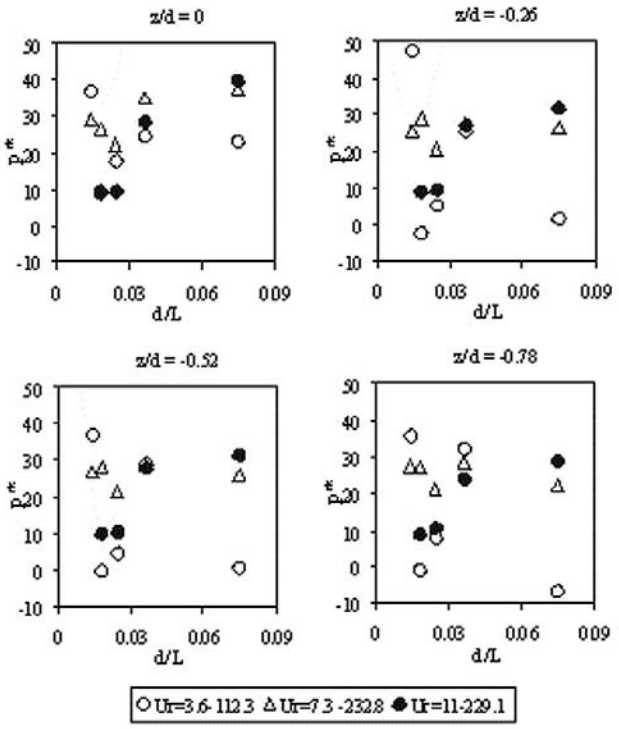

Fig. 6—p* distribution of model (FSS) for various *d/L* and U_r.

Kamikubo *et al.*[5], the continuous change of radius of curvature results in a smooth fluid motion along the curved face of seawall and experiencing pressure variation similar to that experienced by an upright seawall. However, the magnitude of pressure on the model (FSS) is found to be slightly higher. This is due to the surface profile of seawall which directs the flow towards sea, in the process water thrust exerted upon the surface of seawall is be more.

The variation of p* for model (CPS) as a function of *d/L* for U_r range of 3.6 - 229.1 and *z/d* = 0.0, –0.26, –0.52 and –0.78 are shown in Fig. 7. The trend in the pressure variation on model (CPS) is found to be almost similar to that on model (GS). At locations below *z/d* = –0.7, the pressure on model (CPS) is found to be less than for model (VW) and at *z/d* > –0.5, the pressure found to be higher for model (CPS). This is again due to the effect of curvature of model (CPS) as noticed for model (GS), being more flat at that locations, and hence the exerted dynamic pressure is less. At *z/d* = –0.26, the maximum increase in p* for model (CPS), compared to model (VW) is observed to be about 65%.

Run-up analysis

The variations of relative run-up (R_u/H) as a function of *d/L* for models (VW) and (GS) with their

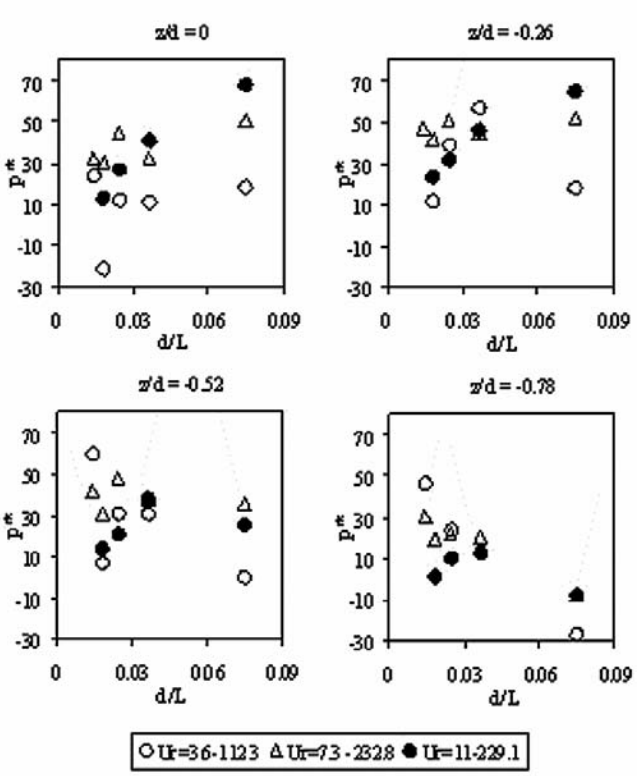

Fig. 7—p* distribution of model (CPS) for various *d/L* and U_r.

toe in a water depth of 0.46 m for U_r ranging between 3.6 - 229.1 are plotted in Fig. 8(a). The (R_u/H) in general is found to decrease with an increase in *d/L*. A comparison of the results for models (VW) and (GS) exhibit that run-up is found to be higher for the curved seawall model (GS). The variations of relative run-up (R_u/H) as a function of *d/L* for models (VW) and (GS) with their toe in a water depth of 0.34 m for U_r ranging between 4.8-301.7 are plotted in Fig. 8(b). The results show that model (GS) experiences higher run-up with a decrease in the water depth. This is due to the shoaling of waves while progressing over the toe of the model and becomes steeper. Thus the curvature of the model (GS) facilitates more energy available for the wave run-up. Further, as the shoreward surface tends to become vertical, the pressure exerted on the wall is also higher. A closer examination of results shows that model (GS) experiences a run-up of about 25% higher compared to model (VW).

When the waves propagate over a curvature of the re-curved seawall, whole or part of its surface is wetted, so the run-up is not significant for re-curved seawall models (FSS) and (CPS). The curvature of the seawall guides the wave towards the sea and hence, the overtopping is avoided.

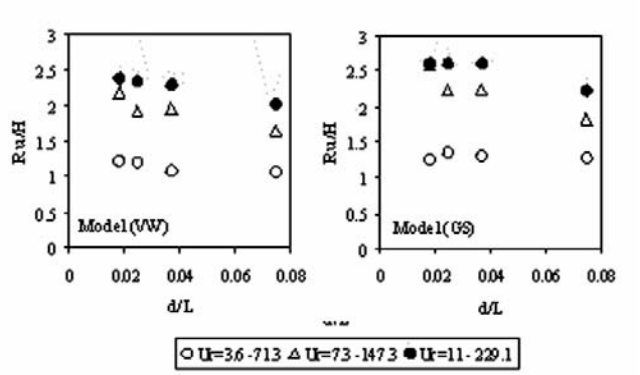

Fig. 8(a)—The variation of run-up (R_u/H) with *d/L* for various U_r in the water depth of 1.0 m.

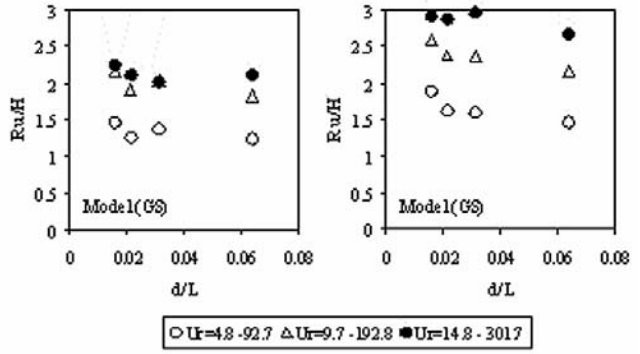

Fig. 8(b)—The variation of run-up (R_u/H) with *d/L* for various U_r in the water depth of 0.88 m.

Regression analysis

The experimental measurements of dynamic pressures are subjected to multiple regression analysis based on least square method. The equations thus arrived for the dependent variable p** = $p_{sh}/\gamma H$ as a function of associated dimensionless parameters; *z/d* and U_r, for the four models are presented below.

Regression equations for dynamic pressures along the depth:

Model - (VW)

$$\frac{p_{sh}}{\gamma H} = -0.0121\frac{z}{d} + 0.0016U_r + 0.6926 \quad \ldots(2)$$

Model - (GS)

$$\frac{p_{sh}}{\gamma H} = 0.0868\frac{z}{d} + 0.0018U_r + 0.8083 \quad \ldots(3)$$

Model - (FSS)

$$\frac{p_{sh}}{\gamma H} = 0.1162\frac{z}{d} + 0.0018U_r + 0.9268 \quad \ldots(4)$$

Model - (CPS)

$$\frac{p_{sh}}{\gamma H} = -0.2921\frac{z}{d} + 0.0021U_r + 1.0298 \quad \ldots(5)$$

Comparisons of the measured with the computed p** for the four models projected in Fig. 9, exhibits a reasonable agreement for all the three curved seawall sections and it is not predicting well for vertical wall model (VW). The correlation coefficients for the above four expressions varies between 0.7 and 0.85. The above equations are derived for all the models over a constant bed slope of 1:30, and for the U_r ranging from 3 to 301.

Models (VW) and (FSS) experience higher pressure than models (GS) and (CPS) at the *z/d* ratios less than –0.5, which is nearer to their toe, and hence the velocity in this region is expected to be less. Hence it is believed that the driving force for inducing scour near the toe of the structure may be less for the models (VW) and (FSS). Even though, the scour is less at model (VW), it

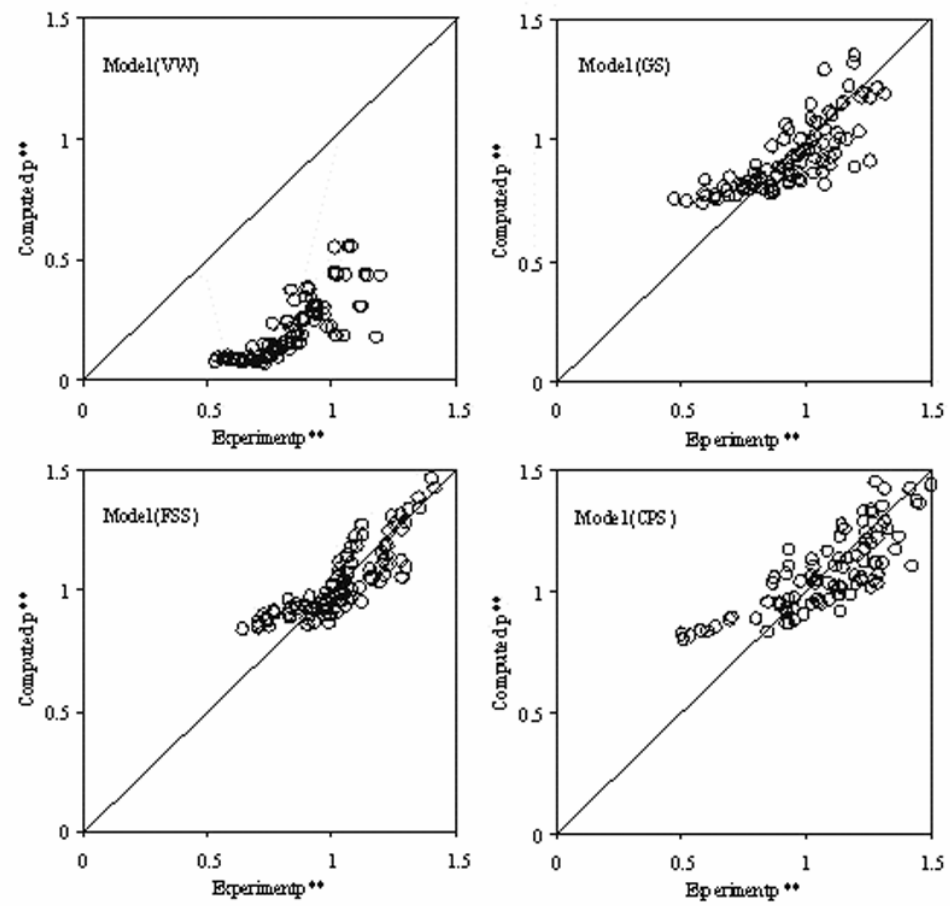

Fig. 9—Regression analysis comparison between experimental and computational values of dynamic pressures.

experiences overtopping at higher *H/d* and *d/L* ratios, which is absent for model (FSS). Hence, model (FSS) is found to be better in terms of lesser disturbance near the toe as well as no overtopping of waves. But the shape of the curvature of model (GS) is not adequate in directing the wave more towards the ocean by the way of dissipation, thereby leading to an increase in the run-up and subsequently requiring a higher crest elevation to avoid overtopping.

Conclusions

A detailed study on the dynamic pressures and run-up of four different shapes of sea wall models was carried out through an experimental program. The salient conclusions drawn from the study are — At relative water depth (*z/d)* = –0.26, the maximum percentage increase in the pressures on models (GS), (FSS) and (CPS) compared to that on (VW) occurring at lower depth to wave length ratio (*d/L)* for Ursell number (U_r) ranging between 3.6-112.3 is about 28%, 47% and 65% respectively. The curvature of model (GS) is found inadequate in directing the wave run-up towards the ocean, there by leading to an increase in the run-up by about 25% compared to that for the vertical seawall model. The results on the other two models (FSS and CPS) have yielded favorable results towards the reduction in the crest elevation, because of its re-curved nature. Both the two models (FSS) and (CPS) can be effectively used even in the places where there is a considerable tidal variation (water level variations). However, model (CPS) is less preferred due to higher velocities near the toe that might induce high scour.

References

1 Kirkgoz S, Impact pressure of breaking waves on vertical and sloping walls, *Ocean Engineering*, 18 (1991) 45-99.

2 Mullar G U & Whittaker T J T, An investigation of breaking wave pressures on inclined wall, *Ocean Engg*., 20 (1993) 349-358.

3 Weber C, Seawall, *United States patent office*, U.S. Pat. 1,971, 324, filed July. 18, 1934, issued Aug. 21, 1934.

4 Murakami K, Irie I & Kamikubo Y, *Experiments on a non-wave overtopping type seawall,* International Conference on Coastal Engineering, (Proceedings of the Twenty-fifth International Conference held in Orlando, Florida) 1996, Vol. 122.

5 Kamikubo Y, Murakami K, Irie I & Hamasaki Y, *Study on Practical Application of a Non-Wave Overtopping Type Seawall,* International Conference on Coastal Engineering, (Proceedings of the Twenty-seventh International Conference held in Sydney) 2000, Vol. 126, pp. 2215-2228.

6 Kamikubo Y, Murakami K, Irie I, Kataoka Y & Takehana N, *Reduction of wave overtopping and water spray with using flaring shaped seawall*, (Proceedings of The Thirteenth International Offshore and Polar Engineering Conference, ISOPE, Honolulu, Hawaii), 2003, Vol. 3, pp. 671-676.

7 Murakami K, Kamikubo Y & Kataoka Y, *Hydraulic Performances of Non-Wave Overtopping type Seawall against Sea Level rise due to Global Warming*, edited by J S Chung, S T Grilli, Naito S & Ma Q, (Proceedings of the Eighteenth International Offshore and Polar Engineering Conference, ISOPE, Vancouver, BC, Canada) 2008, Vol. 3, pp. 706-712.

8 Coastal Engineering Manual, U.S. Army Coastal Engineering Research Centre, 2006.

9 Kamikubo Y, Murakami K, Irie I & Hamasaki Y, Transportation of water spray on non-wave overtopping type seawall, in: *Proceedings of the Twelfth International Offshore and Polar Engineering Conference,* edited by J S Chung, M Sayed, M Kashiwagi, T Setoguchi & S W Hong, (ISOPE, Kitakyushu, Japan,) 2002, Vol. 3, pp. 821-826.